

# Angular momentum content of the $\rho$ -meson in lattice QCD

Leonid Ya. Glozman, C. B. Lang, and Markus Limmer

*Institut für Physik, FB Theoretische Physik, Universität Graz, A-8010 Graz, Austria*

The variational method allows one to study the mixing of interpolators with different chiral transformation properties in the non-perturbatively determined physical state. It is then possible to define and calculate in a gauge-invariant manner the chiral as well as the partial wave content of the quark-antiquark component of a meson in the infrared, where mass is generated. Using a unitary transformation from the chiral basis to the LSJ basis one may extract a partial wave content of a meson. We present results for the ground state of the  $\rho$ -meson using quenched simulations as well as simulations with  $n_f = 2$  dynamical quarks, all for lattice spacings close to 0.15 fm. We point out that these results indicate a simple  ${}^3S_1$ -wave composition of the  $\rho$ -meson in the infrared, like in the SU(6) flavor-spin quark model.

PACS numbers: 11.15.Ha, 12.38.Gc

*1. Motivation.* The composition of hadronic states in quantum field theory is a subtle issue. Whereas in non-relativistic approaches the notion of a wave function and a complete basis of states is well-defined, in quantum field theory beyond the ground state there is no well-defined single hadron, and the state is always a scattering state with superposition of many particle components. A given hadron interpolator couples in principle to all states with its quantum numbers.

Lattice studies of hadrons are typically limited to spectroscopy, static observables like magnetic moments, axial couplings, etc., as well as dynamical observables such as form factors, parton distributions, etc. A challenging task is to reveal the composition of hadrons, i.e., to understand the hadron structure in ab-initio QCD calculations. Of course, in principle any hadron contains a large amount of different Fock components and it is hardly possible to reconstruct on the lattice the complete hadron wave function. Nevertheless, the analyses of the phenomenological data and modeling of hadrons suggest that typically only a few components are the dominant ones. To understand in ab-initio calculations the structure of the leading component in the infrared, i.e., at the scale where hadron mass is generated, would be an important step to improve the insight into hadron structure.

There is a tool to study the hadron wave function on the lattice – the variational method [1, 2] (for a recent, more complete set of references see [3]). The correlation function of a hadron interpolator, which is built from a linear combination of many interpolating operators with correct quantum numbers will single out an optimal signal associated with an exponential decay for large Euclidean time distance. This combination defines the “physical” ground state hadron. In the variational method one chooses a set of interpolators  $\{O_1, O_2, \dots, O_N\}$  that potentially couple to a given hadron and computes the correlation matrix

$$C(t)_{ij} = \langle O_i(t) O_j^\dagger(0) \rangle. \quad (1)$$

If the set is complete enough the eigenvalues of a generalized eigenvalue problem may be related to the eigenstates of the Hamiltonian. Then, if one is interested in reconstructing the leading Fock component of a hadron in the infrared, e.g., the  $\bar{q}q$  component of a meson, one needs interpolators that allow one to define uniquely such a component.

Let us consider the chiral limit of two-flavor mesons. All possible quark-antiquark interpolators for non-exotic mesons can be classified according to representations of the  $SU(2)_L \times SU(2)_R$  and  $U(1)_A$  groups [4, 5]. This basis is complete for a quark-antiquark system provided that there is no explicit excitation of the gluonic field with non-vacuum quantum numbers. Using interpolators that belong to this basis allows one to study the chiral symmetry breaking aspects in a meson. Diagonalizing the cross-correlation matrix one can reconstruct a decomposition of a given meson in terms of different representations of the chiral group. Chiral symmetry breaking in the infrared would mean that the meson wave function has components with different transformation properties with respect to  $SU(2)_L \times SU(2)_R$  and  $U(1)_A$ .

It is also of interest to reconstruct a composition of a meson in terms of the  ${}^{2S+1}L_J$  basis, where  $\mathbf{J} = \mathbf{L} + \mathbf{S}$  are the standard angular momenta. Such a decomposition provides a bridge to the language of the quark model. A priori it is clear that in the heavy quark limit the non-relativistic language of the quark model is nearly adequate. There are well known achievements of the quark model, such as the SU(6) flavor-spin symmetry, which is related to rather large masses of the constituent quarks. These large masses are far from the tiny masses of the current quarks and it is unclear what happens for light quarks. While there is a kind of understanding that successes of the quark model are related to chiral symmetry breaking and that these large masses of constituent quarks arise from the coupling of current quarks to the quark condensate at low momenta, a model-independent and gauge-invariant view on this problem is absent. Then, it would be intriguing to see a

decomposition of the leading quark-antiquark Fock component of a meson in terms of the  $^{2S+1}L_J$  basis in the infrared.

There is a possibility to establish the angular momentum decomposition of the leading quark-antiquark component. Both the chiral basis and the  $^{2S+1}L_J$  basis are complete for a two-particle system. There exists a unitary transformation from the chiral basis to the standard  $^{2S+1}L_J$  basis in the center-of-momentum system [6]. Each of the states in the relativistic chiral basis can be uniquely represented in terms of the allowed  $^{2S+1}L_J$  states. Diagonalizing the cross-correlation matrix in terms of the interpolators with carefully chosen chiral transformation properties, and using this unitary transformation to the  $^{2S+1}L_J$  basis one can reconstruct a partial wave decomposition of the leading Fock component of a meson.

The method is general and can be applied to any meson. Here we use as an example the  $\rho$ -meson. If chiral symmetry is unbroken, then there are two possible states in the chiral basis with the  $\rho$ -meson quantum numbers,  $|(0, 1) + (1, 0); 1 1^{--}\rangle$  and  $|(1/2, 1/2)_b; 1 1^{--}\rangle$ , where  $(0, 1) + (1, 0)$  and  $(1/2, 1/2)_b$  specify two different representations of  $SU(2)_L \times SU(2)_R$  that are compatible with the  $\rho$ -meson quantum numbers  $I, J^{PC} = 1, 1^{--}$  (a subscript  $b$  specifies one of the two different representations  $(1/2, 1/2)_a$  and  $(1/2, 1/2)_b$  [4, 5]). These two representations are a complete set for particles with the quantum numbers of the  $\rho$ -meson. A unitary transformation from the chiral basis to the  $^{2S+1}L_J$  basis takes the form

$$\begin{aligned} |(0, 1) + (1, 0); 1 1^{--}\rangle &= \sqrt{\frac{2}{3}}|1; {}^3S_1\rangle + \sqrt{\frac{1}{3}}|1; {}^3D_1\rangle, \\ |(1/2, 1/2)_b; 1 1^{--}\rangle &= \sqrt{\frac{1}{3}}|1; {}^3S_1\rangle - \sqrt{\frac{2}{3}}|1; {}^3D_1\rangle. \end{aligned} \quad (2)$$

Hence, if we choose two different interpolators with the same spatial content (i.e., with same smearing width of the quarks; its size defines the scale where we probe the hadron) and transformation properties according to  $|(0, 1) + (1, 0); 1 1^{--}\rangle$  and  $|(1/2, 1/2)_b; 1 1^{--}\rangle$ , we will be able to reconstruct the angular momentum content of the  $\bar{q}q$  component. Such interpolators are well-known – the quark bilinears  $\bar{q}\gamma^i\tau q$  and  $\bar{q}\sigma^{0i}\tau q$  [7]. It has been established in lattice simulations that the  $\rho$ -meson couples to both (see, e.g., [8, 9, 10] for quenched and [11] for dynamical simulations). A key property is that these two interpolators have radically different chiral transformation properties. The former one transforms as  $(0, 1) + (1, 0)$  while the latter one belongs to the  $(1/2, 1/2)_b$  representation of  $SU(2)_L \times SU(2)_R$ . Consequently, by diagonalizing the cross-correlation matrix with the  $\bar{q}\gamma^i\tau q$  and  $\bar{q}\sigma^{0i}\tau q$  interpolators we can reconstruct a decomposition of a given eigenstate (i.e., of the ground state  $\rho$ -meson and its excitations) in terms of the possible partial waves in

the infrared.

2. *Analysis of lattice correlators.* For completeness we briefly summarize the features of the variational analysis that allow the decomposition of the ground state properties in the  $\rho$ -channel.

The normalized physical states  $|n\rangle$  propagate in time with

$$\langle n(t)|m(0)\rangle = \delta_{nm}e^{-E^{(n)}t}. \quad (3)$$

The interpolating (lattice) operators  $O_i(t)$  are projected to vanishing spatial momentum and are usually not normalized. We compute the correlation function

$$C(t)_{ij} = \langle O_i(t)O_j^\dagger(0)\rangle = \sum_n a_i^{(n)}a_j^{(n)*}e^{-E^{(n)}t}, \quad (4)$$

with the coefficients giving the overlap of the lattice operator with the physical state,

$$a_i^{(n)} = \langle 0|O_i|n\rangle. \quad (5)$$

For interpolating operators  $O_i$  spanning an orthogonal basis these values would indeed constitute the wave function of state  $|n(0)\rangle$  in that basis.

We assume that the correlation matrix (4) can be approximated by a finite sum over  $N$  states and denote this approximation by  $\widehat{C}(t)_{ij}$ .

It can be shown [1, 2] (for a recent discussion see [3, 12]) that the generalized eigenvalue problem

$$\widehat{C}(t)_{ij}u_j^{(n)} = \lambda^{(n)}(t, t_0)\widehat{C}(t_0)_{ij}u_j^{(n)} \quad (6)$$

allows to recover the correct eigenvalues and eigenvector within some approximation. One finds

$$\lambda^{(n)}(t, t_0) = e^{-E^{(n)}(t-t_0)} \left( 1 + \mathcal{O}\left(e^{-\Delta E^{(n)}(t-t_0)}\right) \right), \quad (7)$$

where  $\Delta E^{(n)}$  may be as small as the distance to the next nearby energy level. In [3] it was pointed out that in an interval  $t_0 \leq t \leq 2t_0$  these contributions are suppressed and leading terms even have  $\Delta E^{(n)}$  equal to the distance to the first neglected energy level  $E_{N+1}$ . At  $t_0$  all eigenvalues are 1 and the eigenvectors are arbitrary.

The eigenvectors come out orthogonal (dual) to the original wave functions  $a^{(n)}$ ,

$$(u^{(n)}, a^{(m)}) \equiv \sum_{i=1}^N u_i^{(n)*} a_i^{(m)} = c^{(m)}\delta_{nm}, \quad (8)$$

and approximate the correct ones. Here  $c^{(m)}$  is a normalization which we get rid off below.

We define a sum of lattice operators

$$\eta^{(n)} \equiv \sum_{i=1}^N u_i^{(n)*} O_i, \quad (9)$$

and find

$$\begin{aligned} \langle 0|\eta^{(n)}|m\rangle &= \sum_{i=1}^N u_i^{(n)*} \langle 0|O_i|m\rangle \\ &= \sum_{i=1}^N u_i^{(n)*} a_i^{(m)} = c^{(n)} \delta_{nm}. \end{aligned} \quad (10)$$

Therefore

$$\eta^{(n)\dagger}|0\rangle = c^{(n)*}|n\rangle. \quad (11)$$

The eigenvector coefficients are related to the composition of the eigenstate in terms of the interpolating operators. The original values  $a_i^{(n)}$  are then

$$\begin{aligned} a_i^{(n)} = \langle 0|O_i|n\rangle &= \frac{1}{c^{(n)*}} \langle 0|O_i \eta^{(n)\dagger}|0\rangle \\ &= \frac{1}{c^{(n)*}} \sum_{j=1}^N u_j^{(n)} \langle 0|O_i O_j^\dagger|0\rangle. \end{aligned} \quad (12)$$

They would agree with  $u_j^{(n)}$  if the interpolators were orthogonal, which they are usually not.

However, with (4) and (8) we find for the large  $t$  behavior (summation convention)

$$\begin{aligned} w_i^{(n)} &\equiv \widehat{C}(t)_{ij} u_j^{(n)} = c^{(n)*} a_i^{(n)} e^{-E^{(n)}t}, \\ (u^{(n)}, w^{(n)}) &= u_i^{(n)*} \widehat{C}(t)_{ij} u_j^{(n)} = c^{(n)*} u_i^{(n)*} a_i^{(n)} e^{-E^{(n)}t} \\ &= |c^{(n)}|^2 e^{-E^{(n)}t}, \end{aligned} \quad (13)$$

and for the ratio for large  $t$

$$\frac{|w_i^{(n)}|^2}{(u^{(n)}, w^{(n)})} = |a_i^{(n)}|^2 e^{-E^{(n)}t}. \quad (14)$$

Assuming asymptotically leading exponential behavior this allows to read off  $|a_i^{(n)}|$  in the asymptotic region.

The ratio

$$\left| \frac{a_i^{(n)}}{a_i^{(m)}} \right|^2 = \left| \frac{\langle 0|O_i(t)|n\rangle}{\langle 0|O_i(t)|m\rangle} \right|^2 \quad (15)$$

tells us how much the interpolating operator  $O_i$  contributes to the eigenstates  $|n\rangle$  and  $|m\rangle$ . This can be used to discuss the ratio of decay constants of various excitations as done in [3, 12, 13].

If we are interested in ratios of couplings of the different lattice operators to the physical states, we may utilize

$$\frac{C(t)_{ij} u_j^{(n)}}{C(t)_{kj} u_j^{(m)}} = \frac{a_i^{(n)}}{a_k^{(m)}}. \quad (16)$$

This ratio tells us how much different interpolating operators contribute to the eigenstate  $|n\rangle$ . This can be used to discuss contributions of, e.g., different representations of the vector meson channel.

TABLE I: Specification of the data used here; for the gauge coupling only the leading value  $\beta_{LW}$  is given,  $m_0$  denotes the bare mass parameter of the CI-action. Further details like the determination of the lattice spacing and the  $\pi$ - and  $\rho$ -masses are found in [15, 16]. For the quenched case and ensemble A we used 100 configurations, for sets B and C we analyzed 200 configurations each. The lattice size is  $16^3 \times 32$ .

Data	$\beta_{LW}$	$a m_0$	$a$ [fm]	$m_\pi$ [MeV]	$m_\rho$ [MeV]
Quenched	7.90	0.04–0.20	0.1480(10)	475–1053	912–1251
dyn.: A	4.70	-0.050	0.1507(17)	526(7)	922(17)
dyn.: B	4.65	-0.060	0.1500(12)	469(4)	897(13)
dyn.: C	4.58	-0.077	0.1440(12)	318(5)	810(28)

3. *Lattice simulation and results.* In a series of papers we have studied the hadron spectrum derived in the quenched case [10, 14, 15] as well as for dynamical fermions [16]. The gauge field action was the Lüscher-Weisz action and the fermions were simulated with the so-called chirally improved (CI) Dirac operator [17, 18].

In these analyses the variational method was used; the hadron interpolators were built from smeared quark sources. Here we refer only to a subset of these results, namely the  $\rho$ -channel ( $J^{PC} = 1^{--}$ ) and restrict ourselves to the four interpolators

$$O_1 = \bar{u}_n \gamma^i d_n, \quad O_2 = \bar{u}_w \gamma^i d_w, \quad (17)$$

$$O_3 = \bar{u}_n \gamma^t \gamma^i d_n, \quad O_4 = \bar{u}_w \gamma^t \gamma^i d_w. \quad (18)$$

Here  $\gamma^i$  is one of the spatial Dirac matrices,  $\gamma_t$  is the  $\gamma$ -matrix in (Euclidean) time direction, and the subscripts  $n$  and  $w$  (for narrow and wide) denote the two smearing widths, 0.25 fm and 0.41 fm, respectively [15].

All results have been obtained on lattices of size  $16^3 \times 32$  with lattice spacing  $a$  close to 0.15 fm (see Table I). The runs A, B and C are for  $n_f = 2$  mass degenerate CI-fermions.

As detailed in [15, 16] it is possible to identify the ground state and the first excited state. In that study we also presented the corresponding eigenvector components ( $u_j^{(1)}$  in our present notation) which were stable over several time slices. Continuing that analyses we now utilize Eq. (16) and determine the ratios  $a_i/a_k$  for the ground state (we have dropped the superscript reference to the physical state), in particular  $a_1/a_3$  and  $a_2/a_4$  which give information on the relative contributions of operators with  $\gamma^i$  compared to  $\gamma^t \gamma^i$ .

We chose the relatively small value  $t_0 = 1$ . Larger values lead to larger errors; however, we found very nice plateau behavior over a range of propagation distance in Euclidean time  $t$ . In Fig. 1 we show the surprising stability of the plateau of the ratio  $a_1/a_3$  for the three data sets obtained for dynamical fermions. We average the values in the range  $3 \leq \Delta t \leq 7$  and show the resulting

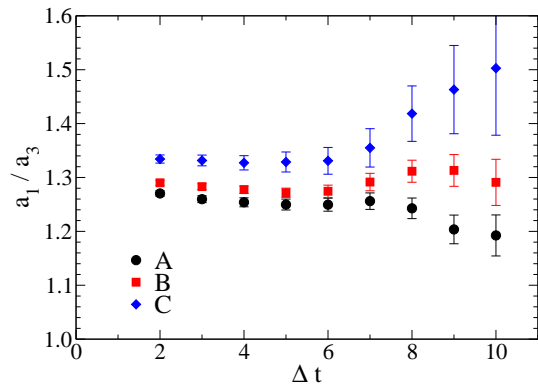


FIG. 1: As an example we show the ratio of the contributions of  $O_1$  vs.  $O_3$  (the narrow-narrow smeared operators) for ensembles A, B and C. All four operators have been included in the correlation matrix. We do not show the points for  $\Delta t \leq t_0 = 1$  and above  $\Delta t = 10$ , where approaching the time-symmetry points the results become statistically unstable. The error bars have been determined with single-elimination jack-knife.

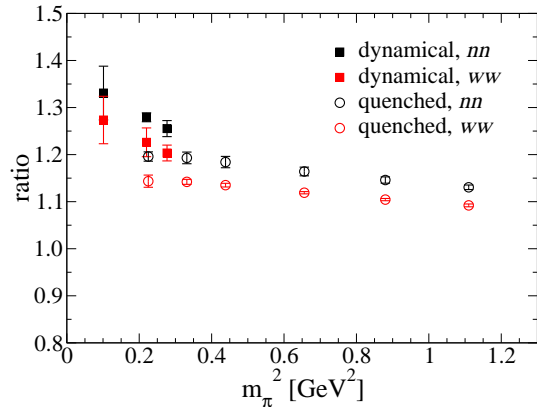


FIG. 2: We show the plateau mean values of the ratios  $a_1/a_3$  and  $a_2/a_4$  for the quenched (circles) and dynamical (filled squares) data sets considered in Table I. For the dynamical data we also have partially quenched results, i.e., with  $m_{valence} > m_{sea}$  (not shown here), which approach the purely quenched values for pion masses above  $\approx 0.7$  GeV. The error bars have been determined with single-elimination jack-knife.

ratio in Fig. 2 for both, the quenched and the dynamical data. We find different behavior towards the chiral limit, indicating the effect of the fermion sea.

Extrapolation towards the physical point indicates a value close to 1.35, i.e., compatible with  $\sqrt{2}$  within the errors. Consequently chiral symmetry is broken such that the  $\bar{q}q$  component of the  $\rho$ -meson is a superposition of the  $(0, 1) + (1, 0)$  and the  $(\frac{1}{2}, \frac{1}{2})_b$  representations with the ratio close to  $\sqrt{2}$ . Inverting the unitary matrix in (2) we then conclude that the physical  $\rho$ -meson in the infrared is almost purely a  $^3S_1$  state. This gives a model-independent and gauge invariant explanation of

the success of the SU(6) flavor-spin symmetry for the  $\rho$ -meson.

This result holds in the infrared where the mass is generated. We probe the chiral and partial wave content of the  $\rho$  wave function at a scale fixed by the smearing size. At higher resolution ( $Q^2 \rightarrow \infty$ ) the  $\beta$ -function approaches zero, the pseudotensor current decouples from the  $\rho$ -meson and the partial wave decomposition should be determined by the  $(0, 1) + (1, 0)$  representation. Such a tendency is indicated in Fig. 2. It is also consistent with the ratio  $\approx 1.6$  obtained in dynamical calculations with point interpolators (i.e., a scale fixed by  $a = 0.114$  fm) in [11].

We thank G. Engel, C. Gattringer and D. Mohler for discussions. L.Ya.G. and M.L. acknowledge support of the Fonds zur Förderung der Wissenschaftlichen Forschung (P19168-N16) and (DK W1203-N08), respectively. The calculations have been performed on the SGI Altix 4700 of the Leibniz-Rechenzentrum Munich and on local clusters at ZID at the University of Graz.

- 
- [1] C. Michael, Nucl. Phys. B **259**, 58 (1985).
  - [2] M. Lüscher and U. Wolff, Nucl. Phys. B **339**, 222 (1990).
  - [3] B. Blossier, M. DellaMorte, G. von Hippel, T. Mendes, and R. Sommer, JHEP **0904**, 094 (2009), arXiv:0902.1265 [hep-lat].
  - [4] L. Y. Glozman, Phys. Lett. B **587**, 69 (2004), hep-ph/0312354.
  - [5] L. Y. Glozman, Phys. Rep. **444**, 1 (2007), hep-ph/0701081.
  - [6] L. Y. Glozman and A. V. Nefediev, Phys. Rev. D **76**, 096004 (2007), arXiv:0704.2673 [hep-ph].
  - [7] T. D. Cohen and X. Ji, Phys. Rev. D **55**, 6870 (1997), hep-ph/9612302.
  - [8] D. Becirevic, V. Lubicz, F. Mescia, and C. Tarantino, JHEP **0305** 007 (2003), hep-lat/0301020.
  - [9] V. M. Braun et al., Phys. Rev. D **68**, 054501 (2003), hep-lat/0306006.
  - [10] T. Burch et al., Phys. Rev. D **73**, 094505 (2006), hep-lat/0601026.
  - [11] C. Allton et al., Phys. Rev. D **78**, 114509 (2008), arXiv:0804.0473 [hep-lat].
  - [12] T. Burch, C. Hagen, C. B. Lang, M. Limmer, and A. Schäfer, Phys. Rev. D **79**, 014504 (2009), arXiv:0809.1103 [hep-lat].
  - [13] T. Burch and C. Ehmman, Nucl. Phys. A **797**, 33 (2007), hep-lat/0701001.
  - [14] T. Burch et al., Phys. Rev. D **70**, 054502 (2004), hep-lat/0405006.
  - [15] C. Gattringer, L. Y. Glozman, C. B. Lang, D. Mohler, and S. Prelovsek, Phys. Rev. D **78**, 034501 (2008), arXiv:0802.2020 [hep-lat].
  - [16] C. Gattringer et al., Phys. Rev. D **79**, 054501 (2009), arXiv:0812.1681 [hep-lat].
  - [17] C. Gattringer, Phys. Rev. D **63**, 114501 (2001), hep-lat/0003005.
  - [18] C. Gattringer, I. Hip, and C. B. Lang, Nucl. Phys. B **597**, 451 (2001), hep-lat/0007042.